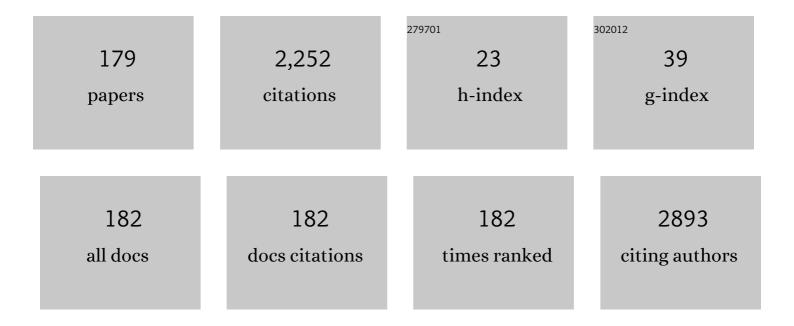
List of Publications by Year in descending order

Source: https://exaly.com/author-pdf/6903098/publications.pdf Version: 2024-02-01



#	Article	IF	CITATIONS
1	Magnetization of Magnetically Inhomogeneous Sr2FeMoO6-l̂´ Nanoparticles. Electronic Materials, 2022, 3, 82-92.	0.9	1
2	Strontium Ferromolybdate-Based Magnetic Tunnel Junctions. Applied Sciences (Switzerland), 2022, 12, 2717. Application of the Quantum-Point-Contact Formalism to Model the Filamentary Conduction in	1.3	2
3	<pre><mmi:math xmins:mmi="http://www.w3.org/1998/Wath/Math/Math/Math/Math/Math/Math/Math/M&lt;/td"><td>1.5</td><td>5</td></mmi:math></pre>	1.5	5
4	Enhancing the luminescence yield of Cr3+ in <b> <i>l²</i> </b> -Ga2O3 by proton irradiation. Applied Physics Letters, 2022, 120, .	1.5	8
5	Tunneling conduction mechanisms in strontium ferromolybdate ceramics with strontium molybdate dielectric intergrain barriers. Journal of Alloys and Compounds, 2021, 860, 158526.	2.8	9
6	Spin-Torque-Triggered Magnetization Reversal in Magnetic Tunnel Junctions with Perpendicular Shape Anisotropy. Physical Review Applied, 2021, 16, .	1.5	5
7	Magnetoelectric Effect in the Bidomain Lithium Niobate/Nickel/Metglas Gradient Structure. Physica Status Solidi (B): Basic Research, 2020, 257, 1900398.	0.7	12
8	Functional Multicomponent Metal Oxide Films Based on Sr, Sn, Fe, and Mo in the Anodic Alumina Matrices. Physica Status Solidi (B): Basic Research, 2020, 257, 1900283.	0.7	4
9	Dynamic magnetic properties of amorphous Fe80B20 thin films and their relation to interfaces. AIP Advances, 2020, 10, 015013.	0.6	7
10	Valence State of Iron and Molybdenum Cations under Conditions of Anionic Deficiency in Sr 2 FeMoO 6– δ. Physica Status Solidi (B): Basic Research, 2020, 257, 1900387.	0.7	2
11	Functional Multicomponent Metal Oxide Films Based on Sr, Sn, Fe, and Mo in the Anodic Alumina Matrices. Physica Status Solidi (B): Basic Research, 2020, 257, 2070018.	0.7	2
12	Advanced Magnetic Oxides. Physica Status Solidi (B): Basic Research, 2020, 257, 2000058.	0.7	0
13	Ar <sup>+</sup> ion irradiation of magnetic tunnel junction multilayers: impact on the magnetic and electrical properties. Journal Physics D: Applied Physics, 2020, 53, 455003.	1.3	6
14	Dual Vibration and Magnetic Energy Harvesting With Bidomain LiNbO <sub>3</sub> -Based Composite. IEEE Transactions on Ultrasonics, Ferroelectrics, and Frequency Control, 2020, 67, 1219-1229.	1.7	22
15	Stabilization of the easy-cone magnetic state in free layers of magnetic tunnel junctions. Physical Review B, 2019, 100, .	1.1	11
16	Metallic filamentary conduction in valence change-based resistive switching devices: the case of TaO <sub>x</sub> thin film with <i>x</i> â^¼ 1. Nanoscale, 2019, 11, 16978-16990.	2.8	16
17	Electrophysical Properties of Sr2FeMoO6–Î′ Ceramics with Dielectric Shells. NATO Science for Peace and Security Series B: Physics and Biophysics, 2019, , 21-40.	0.2	0
18	Defectâ€Induced Effects in Nanomaterials. Physica Status Solidi (B): Basic Research, 2019, 256, 1900181.	0.7	0

#	Article	IF	CITATIONS
19	Formation of epitaxial p-i-n structures on the basis of (In,Fe)Sb and (Ga,Fe)Sb diluted magnetic semiconductors layers. Journal of Magnetism and Magnetic Materials, 2019, 487, 165321.	1.0	8
20	Highly sensitive magnetic field sensor based on a metglas/bidomain lithium niobate composite shaped in form of a tuning fork. Journal of Magnetism and Magnetic Materials, 2019, 486, 165209.	1.0	36
21	Low-Frequency Vibration Energy Harvesting With Bidomain LiNbO <sub>3</sub> Single Crystals. IEEE Transactions on Ultrasonics, Ferroelectrics, and Frequency Control, 2019, 66, 1480-1487.	1.7	23
22	Robustness of ferromagnetism in (In,Fe)Sb diluted magnetic semiconductor to variation of charge carrier concentration. Journal of Magnetism and Magnetic Materials, 2019, 485, 236-243.	1.0	9
23	Smallâ€Angle Neutron Scattering and Magnetically Heterogeneous State in Sr 2 FeMoO 6–Î′. Physica Status Solidi (B): Basic Research, 2019, 256, 1800428.	0.7	6
24	Low-Frequency Vibration Sensor with a Sub-nm Sensitivity Using a Bidomain Lithium Niobate Crystal. Sensors, 2019, 19, 614.	2.1	25
25	Memristive Properties of GaN HEMTs Containing Deepâ€Level Traps. Physica Status Solidi (B): Basic Research, 2019, 256, 1800387.	0.7	4
26	The Role of the Fe/Mo Cations Ordering Degree and Oxygen Nonâ€Stoichiometry on the Formation of the Crystalline and Magnetic Structure of Sr <sub>2</sub> FeMoO <sub>6â^'<i>Î </i></sub> . Physica Status Solidi (B): Basic Research, 2019, 256, 1800278.	0.7	12
27	Low-frequency magnetic sensing by magnetoelectric metglas/bidomain LiNbO <sub>3</sub> long bars. Journal Physics D: Applied Physics, 2018, 51, 214001.	1.3	29
28	Correlation between the transport mechanisms in conductive filaments inside Ta2O5-based resistive switching devices and in substoichiometric TaOx thin films. Applied Physics Letters, 2018, 112, .	1.5	19
29	Ion irradiation-induced easy-cone anisotropy in double-MgO free layers for perpendicular magnetic tunnel junctions. Applied Physics Letters, 2018, 112, .	1.5	14
30	β yclodextrin as a Precursor to Holey Câ€Đoped g <sub>3</sub> N <sub>4</sub> Nanosheets for Photocatalytic Hydrogen Generation. ChemSusChem, 2018, 11, 2681-2694.	3.6	92
31	Magnetoelectric metglas/bidomain <i>y</i> + 140°-cut lithium niobate composite for sensing fT magnetic fields. Applied Physics Letters, 2018, 112, .	1.5	44
32	Magnetic and electric characterizations of sol–gel-derived NaFe(WO4)2 rods. Applied Physics A: Materials Science and Processing, 2018, 124, 1.	1.1	1
33	Equivalent Magnetic Noise in Magnetoelectric Laminates Comprising Bidomain LiNbO <sub>3</sub> Crystals. IEEE Transactions on Ultrasonics, Ferroelectrics, and Frequency Control, 2017, 64, 1102-1119.	1.7	33
34	Synthesis and dielectric properties of ferroelectric-ferrimagnetic PZT-SFMO composites. Modern Electronic Materials, 2017, 3, 26-31.	0.2	5
35	Raman, EPR and ethanol sensing properties of oxygen-Vacancies SrTiO 3- δ compounds. Applied Surface Science, 2017, 426, 386-390.	3.1	54
36	High-temperature intrinsic ferromagnetism in the (In,Fe)Sb semiconductor. Journal of Applied Physics, 2017, 122, .	1.1	25

#	Article	IF	CITATIONS
37	Inhomogeneous free layer in perpendicular magnetic tunnel junctions and its impact on the effective anisotropies and spin transfer torque switching efficiency. Physical Review B, 2017, 96, .	1.1	15
38	Magnetoresistive effect in nanosized strontium ferromolybdate with dielectric interlayers. Modern Electronic Materials, 2016, 2, 106-111.	0.2	2
39	Defect-induced Effects in Nanomaterials. Physica Status Solidi C: Current Topics in Solid State Physics, 2016, 13, 868-869.	0.8	Ο
40	Transfer of spin reorientation in a NdCo <sub>5</sub> /Fe bilayer. Journal Physics D: Applied Physics, 2016, 49, 315002.	1.3	4
41	Dynamic Measurements of Magnetoelectricity in Metglas-Piezocrystal Laminates. Nanoscience and Technology, 2016, , 227-265.	1.5	4
42	Engineering the Magnetoelectric Response in Piezocrystal-Based Magnetoelectrics: Basic Theory, Choice of Materials, Model Calculations. Nanoscience and Technology, 2016, , 189-226.	1.5	1
43	Charge ordering and magnetic properties in nanosized Sr <sub>2</sub> FeMoO <sub>6–<i>δ</i></sub> powders. Physica Status Solidi (B): Basic Research, 2016, 253, 2160-2166.	0.7	18
44	Electrical transport properties of a superconductor-ferrimagnet composite in applied magnetic fields. Physica Status Solidi (B): Basic Research, 2016, 253, 2154-2159.	0.7	0
45	Ionâ€beam induced effects in multiâ€layered semiconductor systems. Physica Status Solidi (B): Basic Research, 2016, 253, 2099-2109.	0.7	3
46	Field―and irradiationâ€induced phenomena in memristive nanomaterials. Physica Status Solidi C: Current Topics in Solid State Physics, 2016, 13, 870-881.	0.8	92
47	Splitting of standing spin-wave modes in circular submicron ferromagnetic dot under axial symmetry violation. Scientific Reports, 2016, 5, 18480.	1.6	10
48	Iron incorporation into magnesium aluminosilicate glass network under fast laser floating zone processing. Ceramics International, 2016, 42, 2693-2698.	2.3	11
49	Resistive switching and impedance spectroscopy in SiO -based metal-oxide-metal trilayers down to helium temperatures. Vacuum, 2015, 122, 293-299.	1.6	5
50	Defect-induced effects in nanomaterials. Physica Status Solidi C: Current Topics in Solid State Physics, 2015, 12, 9-9.	0.8	1
51	Anisotropy of the magnetoelectric effect in tri-layered composites based on single-crystalline piezoelectrics. Vacuum, 2015, 122, 286-292.	1.6	16
52	Influence of electron irradiation on p-n junctions in SiGe superlattices. Physica Status Solidi (B): Basic Research, 2015, 252, 153-158.	0.7	0
53	Enhanced radiation hardness of InAs/InP quantum wires. Physica Status Solidi (B): Basic Research, 2015, 252, 134-138.	0.7	1
54	Interplay of Superstructural Ordering and Magnetic Properties of the Sr <sub>2</sub> FeMoO <sub>6–<i>δ</i></sub> Double Perovskite. Science of Advanced Materials, 2015, 7, 446-454.	0.1	12

#	Article	IF	CITATIONS
55	FMR study of carbon nanotubes filled with Fe3O4 nanoparticles. Journal of Magnetism and Magnetic Materials, 2014, 358-359, 44-49.	1.0	16
56	Spin relaxation in inhomogeneous quantum dot arrays studied by electron spin resonance. Physical Review B, 2014, 89, .	1.1	10
57	Anomalous Hall effect in two-phase semiconductor structures: The role of ferromagnetic inclusions. Physical Review B, 2014, 90, .	1.1	12
58	Dynamic exchange via spin currents in acoustic and optical modes of ferromagnetic resonance in spin-valve structures. Physical Review B, 2014, 89, .	1.1	18
59	Direct and converse magnetoelectric effects in Metglas/LiNbO3/Metglas trilayers. Journal of Applied Physics, 2013, 114, .	1.1	23
60	Resonant and non-resonant microwave absorption as a probe of the magnetic dynamics and switching in spin valves. Journal of Applied Physics, 2013, 114, 023906.	1.1	2
61	Radiation effects in Si-Ge quantum size structure (Review). Semiconductors, 2013, 47, 217-227.	0.2	8
62	Room temperature structure and multiferroic properties in Bi0.7La0.3FeO3 ceramics. Journal of Alloys and Compounds, 2013, 554, 97-103.	2.8	32
63	Magnetic anisotropy of epitaxial zinc ferrite thin films grown by pulsed laser deposition. Thin Solid Films, 2013, 527, 273-277.	0.8	15
64	NiFe/CoFe/Cu/CoFe/MnIr spin valves studied by ferromagnetic resonance. Journal of Applied Physics, 2013, 113, 17D713.	1.1	6
65	Synthesis and dielectric properties of Pb0.85Ba0.25Zr0.53Ti0.47O3compounds with nano-inclusions of Cu and Ni. Physica Status Solidi C: Current Topics in Solid State Physics, 2013, 10, 640-645.	0.8	2
66	Microprobe analysis, iono- and photo-luminescence of Mn2+ activated ZnGa2O4 fibres. Nuclear Instruments & Methods in Physics Research B, 2013, 306, 195-200.	0.6	12
67	Defect-induced Effects in Nanomaterials. Physica Status Solidi C: Current Topics in Solid State Physics, 2013, 10, 601-602.	0.8	1
68	Charge transfer processes and magnetoresistance in strontium ferromolybdate with dielectric barriers. Physica Status Solidi (B): Basic Research, 2013, 250, 825-830.	0.7	2
69	Spectroscopy of radiation defects in rutile TiO <sub>2</sub> . Physica Status Solidi (B): Basic Research, 2013, 250, 843-849.	0.7	2
70	Modeling Exchange—Spring Layered Systems With Perpendicular Anisotropy Using Ferromagnetic Resonance Measurements. IEEE Transactions on Magnetics, 2012, 48, 4081-4084.	1.2	2
71	Probing the Quality of Ni Filled Nanoporous Alumina Templates by Magnetic Techniques. Journal of Nanoscience and Nanotechnology, 2012, 12, 7486-7490.	0.9	13
72	Experimental Evidence and Modified Growth Model of Alloying in In <i><sub>x</sub></i> Ga <sub>1–<i>x</i></sub> As Nanowires. Journal of Physical Chemistry C, 2012, 116, 24777-24783.	1.5	14

#	Article	IF	CITATIONS
73	Ferromagnetic resonance and magnetooptic study of submicron epitaxial Fe(001) stripes. Journal of Applied Physics, 2012, 111, .	1.1	5
74	Structural, optical and magnetic resonance properties of TiO2 fibres grown by laser floating zone technique. Applied Surface Science, 2012, 258, 9143-9147.	3.1	13
75	Reaction processes in a ZnO+1%Gd2O3 powder mixture during mechanical and laser processing. Materials Science and Engineering B: Solid-State Materials for Advanced Technology, 2012, 177, 1417-1422.	1.7	2
76	Superferromagnetism and coercivity in Co-Al2O3 granular films with perpendicular anisotropy. Journal of Applied Physics, 2012, 111, 123915.	1.1	30
77	Magnetoelectric coupling in multiferroic heterostructure of rf-sputtered Ni–Mn–Ga thin film on PMN–PT. Journal of Magnetism and Magnetic Materials, 2012, 324, 1882-1886.	1.0	12
78	Structure and magnetic properties of Cd doped copper ferrite. Journal of Alloys and Compounds, 2011, 509, 7585-7590.	2.8	16
79	Spin Dynamics in Two-Dimensional Arrays of Quantum Dots with Local Ordering of Nanoclusters. , 2011, , .		0
80	Faraday effect in ZnO:Mn thin films. AIP Conference Proceedings, 2011, , .	0.3	0
81	Interplay between phase formation mechanisms and magnetism in the Sr <sub>2</sub> FeMoO <sub>6–δ</sub> metalâ€oxide compound. Crystal Research and Technology, 2011, 46, 463-469.	0.6	15
82	Study of structural and ferromagnetic properties of pure and Cd doped copper ferrite. Journal of Physics and Chemistry of Solids, 2011, 72, 862-868.	1.9	20
83	Enhanced ferroelectric, magnetic and magnetoelectric properties of Bi1â^'xCaxFe1â^'xTixO3 solid solid solutions. Solid State Communications, 2011, 151, 536-540.	0.9	41
84	Structure and Magnetic Properties of Nanostructured Pd–Fe Thin Films Produced by Pulse Electrodeposition. Journal of Nanoscience and Nanotechnology, 2011, 11, 8907-8911.	0.9	7
85	Influence of Ge content on the optical properties ofXandWcenters in dilute Si-Ge alloys. Physical Review B, 2011, 84, .	1.1	16
86	Spin dynamics in two-dimensional arrays of quantum dots with different shapes. Journal of Physics: Conference Series, 2010, 245, 012052.	0.3	0
87	Room temperature paramagnetism of ZnO:Mn films grown by RF-sputtering. Thin Solid Films, 2010, 518, 4612-4614.	0.8	7
88	Ferromagnetic resonance on metal nanocrystals in Fe and Ni implanted ZnO. Journal of Applied Physics, 2010, 107, 09B518.	1.1	6
89	Low Temperature Deposition of Ferromagnetic Ni-Mn-Ga Thin Films From Two Different Targets via rf Magnetron Sputtering. Materials Research Society Symposia Proceedings, 2010, 1250, 1.	0.1	2
90	Magnetic properties of amorphous Co0.74Si0.26â^•Si multilayers with different numbers of periods. Low Temperature Physics, 2010, 36, 821-825.	0.2	0

#	Article	IF	CITATIONS
91	Mechanisms of manganese-assisted non-radiative recombination in Cd(Mn)Se/Zn(Mn)Se quantum dots. Journal of Physics Condensed Matter, 2010, 22, 355306.	0.7	12
92	Rhombohedral-to-orthorhombic transition and multiferroic properties of Dy-substituted BiFeO3. Journal of Applied Physics, 2010, 108, .	1.1	86
93	Defect-induced ferromagnetism in undoped and Mn-doped zirconia thin films. Physical Review B, 2010, 82, .	1.1	65
94	Ion Beam Synthesis of Transition Metal Nanoclusters in Silicon. , 2009, , .		1
95	Structural and optical properties of Zn0.9Mn0.1O/ZnO core-shell nanowires designed by pulsed laser deposition. Journal of Applied Physics, 2009, 106, .	1.1	13
96	EFFECT OF <font>Mn</font> IONS ON SPIN RELAXATION AND LIFE-TIME OF <font>e</font> - <font>h</font> COMPLEXES IN <font>CdSe</font> / <font>ZnSe</font> / <font>ZnMnSe</font> QUANTUM DOTS. International Journal of Modern Physics B, 2009, 23, 2984-2988.	1.0	3
97	Optical study of strained double Ge/Si quantum dot layers. IOP Conference Series: Materials Science and Engineering, 2009, 6, 012018.	0.3	2
98	Ferromagnetic semiconductor InMnAs layers grown by pulsed laser deposition on GaAs. Journal Physics D: Applied Physics, 2009, 42, 035006.	1.3	6
99	Magnetic and structural properties of transition metal doped zincâ€oxide nanostructures. Physica Status Solidi (B): Basic Research, 2009, 246, 766-770.	0.7	10
100	Asymmetry effect on the spin relaxation in quantum dot structures. Physica Status Solidi C: Current Topics in Solid State Physics, 2009, 6, 833-836.	0.8	0
101	Doping strategies for increased performance in BiFeO3. Journal of Magnetism and Magnetic Materials, 2009, 321, 1692-1698.	1.0	161
102	Raman scattering on overtones of fully symmetric LO phonons in Zn0.9Mn0.1O nanocrystals under resonance excitation conditions. Technical Physics Letters, 2009, 35, 1086-1089.	0.2	3
103	Optical and structural properties of ZnO nanorods grown by pulsed laser deposition without a catalyst. Technical Physics, 2009, 54, 1607-1611.	0.2	5
104	Ion beam synthesis of Mn/Sb clusters in silicon. Journal Physics D: Applied Physics, 2009, 42, 035406.	1.3	4
105	Photoluminescence and Raman study of a tensilely strained Si type-II quantum well on a relaxed SiGe graded buffer. IOP Conference Series: Materials Science and Engineering, 2009, 6, 012023.	0.3	1
106	SYNTHESIS AND CHARACTERIZATION OF NANOGRAINED <font>PZT</font> - <font>NiFe</font> <sub>2</sub> <font>O</font> <sub>4</sub> - <font>PZT</font> SANDWICHED LAYERS. , 2009, , .		0
107	Magnetic properties of MnP nanowhiskers grown by MBE. Physica E: Low-Dimensional Systems and Nanostructures, 2008, 40, 2037-2039.	1.3	7
108	Electronic properties of Ge islands embedded in multilayer and superlattice structures. Thin Solid Films, 2008, 517, 303-305.	0.8	2

#	Article	IF	CITATIONS
109	MBE growth of Ge/Si quantum dots upon low-energy pulsed ion irradiation. Thin Solid Films, 2008, 517, 309-312.	0.8	7
110	Radiation hardness of GeSi heterostructures with thin Ge layers. Materials Science and Engineering B: Solid-State Materials for Advanced Technology, 2008, 147, 191-194.	1.7	7
111	Ferromagnetic resonance of ultrathin Coâ^•Ag superlattices on Si(111). Journal of Applied Physics, 2008, 103, 07B527.	1.1	6
112	Radiation Effects in Quantum Dot Structures. , 2008, , 392-447.		9
113	Influence of the strong magnetocrystalline anisotropy on the magnetocaloric properties of MnP single crystal. Physical Review B, 2008, 77, .	1.1	62
114	Coexistence of spontaneous ferroelectricity and weak ferromagnetism in Bi <sub>0.8</sub> Pb <sub>0.2</sub> FeO <sub>2.9</sub> perovskite. Journal of Physics Condensed Matter, 2008, 20, 155207.	0.7	18
115	Spin resonance of electrons localized on <mmi:math xmlns:mml="http://www.w3.org/1998/Math/MathML" display="inline"&gt; <mml:mrow> <mml:mi mathvariant="normal"&gt;Ge <mml:mo> â^•</mml:mo> <mml:mi mathvariant="normal"&gt;Si </mml:mi </mml:mi </mml:mrow> quantum dots. Physical Review B, 2008,</mmi:math 	1.1	24
116	Heterovalent A-site doping of multiferroic BiFeO3. , 2008, , .		0
117	Further insight into the temperature quenching of photoluminescence from InAsâ^•GaAs self-assembled quantum dots. Journal of Applied Physics, 2008, 103, .	1.1	22
118	Surface modification of Co-doped ZnO nanocrystals and its effects on the magnetic properties. Journal of Applied Physics, 2008, 103, .	1.1	18
119	OPTICAL AND STRUCTURAL ANALYSIS OF Ge/Si QUANTUM DOTS GROWN ON A Si(001) SURFACE COVERED WITH A SiO2 SUB-MONOLAYER. International Journal of Nanoscience, 2007, 06, 245-248.	0.4	0
120	Electron Paramagnetic Resonance Characterization of Mn- and Co-Doped ZnO Nanowires. AIP Conference Proceedings, 2007, , .	0.3	1
121	Electron paramagnetic resonance in transition metal-doped ZnO nanowires. Journal of Applied Physics, 2007, 101, 024324.	1.1	33
122	Ion beam synthesis of Mn/As-based clusters in silicon. Nuclear Instruments & Methods in Physics Research B, 2007, 257, 90-93.	0.6	4
123	MBE growth of vertically ordered Ge quantum dots on Si. Physica Status Solidi C: Current Topics in Solid State Physics, 2007, 4, 262-264.	0.8	2
124	Ferromagnetic Resonance and Hall Effect Characterization of GaMnSb Layers. Journal of Superconductivity and Novel Magnetism, 2007, 20, 399-403.	0.8	10
125	Effect Of Light Illumination On The Conductivity Of Tunnel-coupled Ge/Si Quantum Dots. AIP Conference Proceedings, 2007, , .	0.3	1
126	Hopping magnetoresistance in two-dimensional arrays of Ge/Si quantum dots. Physica Status Solidi C: Current Topics in Solid State Physics, 2006, 3, 296-299.	0.8	4

#	Article	IF	CITATIONS
127	Influence of matrix defects on the photoluminescence of InAs self-assembled quantum dots. Physica Status Solidi (A) Applications and Materials Science, 2006, 203, 1348-1352.	0.8	6
128	RBS/channeling study of buried Ge quantum dots grown in a Si layer. Nuclear Instruments & Methods in Physics Research B, 2006, 249, 462-465.	0.6	5
129	Influence of defects on the optical and structural properties of Ge dots embedded in an Si/Ge superlattice. Journal of Luminescence, 2006, 121, 417-420.	1.5	11
130	Ferromagnetism and ferromagnetic resonance in Mn and As co-implanted Si and GaAs. Materials Science and Engineering B: Solid-State Materials for Advanced Technology, 2006, 126, 148-150.	1.7	11
131	Damage behaviour of GaAs/AlAs multilayer structures. Nuclear Instruments & Methods in Physics Research B, 2006, 249, 890-893.	0.6	1
132	Effect of Ge doping on the creation of luminescent radiation defects in MBE Si. Nuclear Instruments & Methods in Physics Research B, 2006, 248, 127-132.	0.6	3
133	Photoconduction in tunnel-coupled Ge/Si quantum dot arrays. Journal of Experimental and Theoretical Physics, 2006, 103, 269-277.	0.2	10
134	Ferromagnetism and Ferromagnetic Resonance in Mn Implanted Si and GaAs. Materials Science Forum, 2006, 514-516, 280-283.	0.3	0
135	Ion Beam Analysis of Ge/Si Dots Grown on Ultrathin SiO <sub>2</sub> Interlayers. Materials Science Forum, 2006, 514-516, 1121-1124.	0.3	0
136	Optical and structural study of Ge/Si quantum dots on Si(100) surface covered with a thin silicon oxide layer. Materials Science and Engineering B: Solid-State Materials for Advanced Technology, 2005, 124-125, 462-465.	1.7	6
137	Low-temperature molecular beam epitaxy of Ge on Si. Materials Science in Semiconductor Processing, 2005, 8, 35-39.	1.9	3
138	High resolution backscattering studies of nanostructured magnetic and semiconducting materials. Nuclear Instruments & Methods in Physics Research B, 2005, 241, 454-458.	0.6	13
139	Morphological Transformation of a Germanium Layer Grown on a Silicon Surface by Molecular-Beam Epitaxy at Low Temperatures. Physics of the Solid State, 2005, 47, 71.	0.2	2
140	Structural Characterization and Luminescence of Ge/Si Quantum Dots. Materials Science Forum, 2004, 455-456, 540-544.	0.3	1
141	The electronic structure and magnetic properties of transition metal-doped silicon carbide. Journal of Physics Condensed Matter, 2004, 16, 1761-1768.	0.7	48
142	Orientation effects in the electronic and optical properties of germanium quantum wires. Physical Review B, 2004, 70, .	1.1	38
143	Pulsed laser annealing of Si–Ge superlattices. Materials Science and Engineering C, 2003, 23, 19-22.	3.8	6
144	Carrier dynamics in particle-irradiated InGaAs/GaAs quantum dots. Physica Status Solidi C: Current Topics in Solid State Physics, 2003, 0, 1177-1180.	0.8	1

#	Article	IF	CITATIONS
145	Influence of defects on the luminescence of Ge/Si quantum dots. Physica Status Solidi C: Current Topics in Solid State Physics, 2003, 0, 1267-1270.	0.8	11
146	Photoexcitation electron paramagnetic resonance studies on nickel-related defects in diamond. Journal of Physics Condensed Matter, 2003, 15, 2493-2505.	0.7	8
147	Radiation hardness of InGaAs/GaAs quantum dots. Applied Physics Letters, 2003, 82, 1941-1943.	1.5	47
148	The effect of high-pressure–high-temperature annealing on paramagnetic defects in diamond. Journal of Physics Condensed Matter, 2003, 15, S2941-S2949.	0.7	6
149	SELF-ORGANIZATION PHENOMENA IN PULSED LASER ANNEALED Si/Ge SUPERLATTICES. , 2003, , .		Ο
150	INTRADOT CARRIER RELAXATION IN RADIATION-DAMAGED <font>InGaAs</font> / <font>GaAs</font> QUANTUM DOT HETEROSTRUCTURES. , 2003, , .		0
151	Annealing study of the formation of nickel-related paramagnetic defects in diamond. Diamond and Related Materials, 2002, 11, 623-626.	1.8	20
152	Photo-EPR studies on the AB3 and AB4 nickel-related defects in diamond. Physica B: Condensed Matter, 2001, 308-310, 589-592.	1.3	3
153	Enhanced Radiation Hardness of InAs/GaAs Quantum Dot Structures. Physica Status Solidi (B): Basic Research, 2001, 224, 93-96.	0.7	40
154	Evaluation of the infrared absorption in nm-thick heavily boron-doped Si1-xGex layers on silicon. Journal of Materials Science: Materials in Electronics, 2001, 12, 241-243.	1.1	0
155	Coherent amorphization of Ge/Si multilayers with ion beams. Nuclear Instruments & Methods in Physics Research B, 2001, 178, 279-282.	0.6	2
156	Determination of the W8 and AB5 defect levels in the diamond gap. Journal of Physics Condensed Matter, 2001, 13, 8957-8964.	0.7	12
157	Enhanced radiation hardness of quantum dot lasers to high energy proton irradiation. Electronics Letters, 2001, 37, 174.	0.5	66
158	INFLUENCE OF ELECTRON IRRADIATION ON CARRIER RECOMBINATION AND INTRADOT RELAXATION IN <font>InGaAs</font> / <font>GaAs</font> QUANTUM DOT STRUCTURES., 2001, , .		0
159	New paramagnetic centers in annealed high-pressure synthetic diamond. Diamond and Related Materials, 2000, 9, 1057-1060.	1.8	20
160	Defects incorporating Ge atoms in irradiated Si:Ge. Physica B: Condensed Matter, 1999, 273-274, 271-274.	1.3	11
161	New paramagnetic defects in synthetic diamonds grown using nickel catalyst. Physica B: Condensed Matter, 1999, 273-274, 651-654.	1.3	13
162	Ion beam induced structural transformations in SimGen superlattices. Nuclear Instruments & Methods in Physics Research B, 1998, 136-138, 1057-1061.	0.6	3

#	Article	IF	CITATIONS
163	Amorphization Mechanism of Si/Ge Superlattices Upon Ion Implantation. Materials Research Society Symposia Proceedings, 1998, 540, 91.	0.1	2
164	On the Amorphization of the Si/Ge Superlattices upon Ion Bombardement. Materials Science Forum, 1997, 248-249, 289-294.	0.3	5
165	Luminescence of copper-aluminum diselenide. Semiconductors, 1997, 31, 315-318.	0.2	0
166	RADIATION EFFECTS IN SI/Ge NANOSTRUCTURES. , 1997, , .		1
167	Hydrogen effects on the electrical and optical properties of γ-irradiated n-type GaAs epilayers. Nuclear Instruments & Methods in Physics Research B, 1996, 108, 65-69.	0.6	1
168	Photoluminescence of gallium phosphide epitaxial layers doped with rare-earth elements. Journal of Applied Spectroscopy, 1996, 63, 283-285.	0.3	0
169	Influence of electron irradiation and annealing on the photoluminescence of Si/Ge superlattices and Si/Ge quantum wells. Journal of Crystal Growth, 1996, 167, 502-507.	0.7	8
170	Exciton transitions in photoluminescence spectra of AIAs/GaAs superlattices. Journal of Applied Spectroscopy, 1994, 61, 613-616.	0.3	0
171	The influence of isochronous annealing upon the near-band-edge photoluminescence spectra of the electron-irradiated n-InP. Solid State Communications, 1993, 85, 525-527.	0.9	8
172	Defect-Impurity Interaction in Irradiated n-GaAs. Defect and Diffusion Forum, 1993, 103-105, 51-56.	0.4	0
173	Defect- Impurity Interaction in Irradiated n-GaAs. Materials Research Society Symposia Proceedings, 1992, 262, 603.	0.1	2
174	Rapid Thermal Annealing of Neutron Transmutation Toped Czochralski Silicon. Materials Research Society Symposia Proceedings, 1992, 262, 731.	0.1	0
175	Near-edge luminescence of irradiated silicon. The effect of the form of irradiation and of the annealing temperature. Journal of Applied Spectroscopy, 1989, 51, 797-804.	0.3	1
176	Investigations of Radiation Damage Production in Ion Implanated Silicon. Physica Status Solidi A, 1982, 69, 603-614.	1.7	23
177	EPR studies of point defect and amorphous phase production during ion implantation in Silicon. Radiation Effects, 1979, 42, 23-28.	0.4	18
178	ESR line share study of amorphous centres in ion implanted silicon. Physica Status Solidi A, 1978, 50, K209-K212.	1.7	7
179	Study of SiGe Alloys with Different Germanium Concentrations Implanted with Mn and As Ions. Materials Science Forum, 0, 587-588, 298-302.	0.3	0